ISSN 2616-5775 Vol. 4, Issue 6: 59-66, DOI: 10.25236/AJCIS.2021.040610

Kinematics analysis and simulation of flapping mechanism of two-stage flapping-wing aircraft

Yanjing Wu, Chengwei Zhang

China University of Petroleum-Beijing at Karamay, Karamay, China

Abstract: *In order to improve the flight performance of the flapping-wing aircraft, a two-stage foldable bionic flapping-wing mechanism is designed in this paper with reference to the flight motion characteristics of large birds. Firstly, the kinematic model of the flapping-wing mechanism is established by kinematic analysis, and the relationship equation between flapping angle and input angle and rod length is derived. Then, the three-dimensional model of the flapping-wing wing configuration is built in SolidWorks, and its output motion is obtained by ADAMS simulation to verify the theoretical analysis. The results show that the designed flapping-wing mechanism has a minimum transmission angle of* $\Gamma_{min} = 48.6°$ *and has good force transmission performance. The upper flapping limit of the inner wing is* $\varphi_{max} = 45°$ *and the lower flapping limit is* $\varphi_{min} = -5°$*; the upper flapping limit of the outer wing mechanism is* $\varphi_{max} = 46°$ *and the lower flapping limit is* $\varphi_{min} = -28°$*, which are consistent with the flight motion parameters of large birds.*

Keywords: *two-stage flapping-wing mechanism, kinematics analysis, ADAMS*

1. Introduction

The flapping-wing aircraft is a new type of aircraft designed and manufactured based on the principles of bionics, imitating the flying methods of insects and birds in nature. At present, the technology of fixed-wing and rotary-wing aircraft is already at a very mature stage, but when the size of the aircraft is reduced to the miniature level, the aerodynamic performance of traditional fixed-wing and rotary-wing aircraft is greatly reduced. The flapping-wing aircraft that imitates birds and insects has a low Reynolds number flow and can generate a high lift mechanism [1~3]. It has the advantages of high aerodynamic efficiency, convenient take-off and landing, and moderate speed [4], So that it has better aerodynamic performance, has become a research hotspot at home and abroad.

After observing the flight movements of large birds, it is found that while their wings are flapping up and down, they also bend in the span direction. However, most of the plane-link flapping wing mechanisms that have been launched can only achieve the up and down flapping of the wings [5]. Therefore, in order to better imitate the flight of birds without making the flapping-wing mechanism too complicated, this paper designs a two-stage foldable flapping-wing mechanism. Kinematic analysis and ADAMS simulation show that it has good aerodynamic characteristics.

2. Flapping wing mechanism design

By observing the wing structure and flight movements of large bird seagulls [6], this paper adds a two-bar and three-pole group on the basis of the double-crank and double-rocker mechanism, and designs a two-stage foldable bionic flapping-wing mechanism as shown in Fig. 1. The two-stage flapping wing mechanism is divided into an inner wing and an outer wing, and the movement process of the left and right wings is completely symmetrical. With a two-stage wing structure, the effective force area of the wing relative to the airflow can be adjusted during flight, so as to better imitate the flight of a seagull.

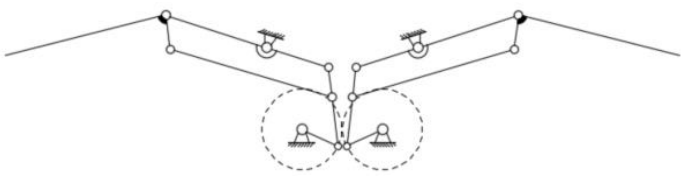

Figure 1: Schematic diagram of flapping mechanism

ISSN 2616-5775 Vol. 4, Issue 6: 59-66, DOI: 10.25236/AJCIS.2021.040610

In order to determine whether the mechanism has a definite movement [7, 8], the degree of freedom of the crank-rocker mechanism is calculated as:

$$F = 3n - 2P_L - P_H \tag{1}$$

In formula (1), n is the number of movable components, P_L is the low number of pairs in the organization, and P_H is the high number of pairs. In the crank-rocker mechanism, the number of movable members is $n = 3$, the number of low pairs is $P_L = 4$, and the number of high pairs is $P_H = 0$. So the degree of freedom of the crank-rocker mechanism is $F = 1$. The degree of freedom of the two-stage rod group is 0, so the degree of freedom of the single-sided flapping wing mechanism is 1.

3. Kinematics analysis of flapping mechanism

3.1. Determination of the size of each rod

Since the left and right flapping wing mechanisms are symmetrical in the vertical plane, the right side of the mechanism is selected as the research object for analysis to facilitate the study. The right flapping mechanism consists of inner wing BCG and outer wing FGH, as shown in Fig. 2.

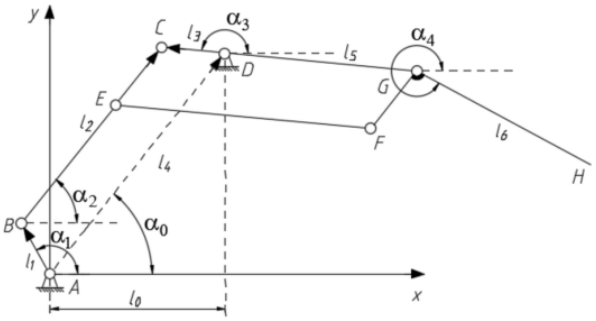

Figure 2: Schematic diagram of one-sided flapping mechanism

The rods CE, EF, FG and GC form a parallelogram mechanism. In order to make the inner and outer wings of the flapping-wing mechanism basically lie on the same horizontal line during the downward flapping process to increase the force area of the wing, the outer wings should be bent as much as possible to reduce the resistance during the upward flapping process, which can be set as $\angle FGH = 75°$[9]. From the geometric relationship in Fig. 2, it can be obtained:

$$\alpha_0 = \arccos\left(\frac{l_0}{l_4}\right) \tag{2}$$

Fig. 3 is a schematic diagram of the mechanism when the crank turns to the two extreme positions, where the upper flapping limit angle and the lower flapping limit angle of the flapping wing mechanism are φ_{max} and φ_{min} respectively.

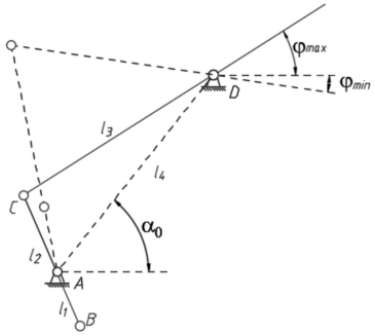

Figure 3: Diagram of flutter limit position

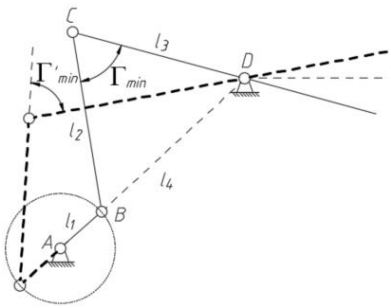

Figure 4: Position diagram of minimum transmission Angle

It can be obtained from geometric relations in Fig. 3:

ISSN 2616-5775 Vol. 4, Issue 6: 59-66, DOI: 10.25236/AJCIS.2021.040610

$$\varphi_{\max} = \alpha_0 - \arccos\left(\frac{{l_3}^2 + {l_4}^2 - (l_2 - l_1)^2}{2l_3 l_4}\right) \tag{3}$$

$$\varphi_{\min} = \arccos\left(\frac{{l_3}^2 + {l_4}^2 - (l_2 + l_1)^2}{2l_3 l_4}\right) - \alpha_0 \tag{4}$$

The flapping amplitude of the flapping mechanism is:

$$\varphi = \varphi_{\max} + \varphi_{\min} \tag{5}$$

In Fig. 4, when the crank and the frame coincide with each other, the minimum transmission angle is:

$$\Gamma_{\min} = \arccos\left(\frac{{l_2}^2 + {l_3}^2 - (l_4 - l_1)^2}{2l_2 l_3}\right) \tag{6}$$

When the crank and the frame are straightened and collinear, the minimum transmission angle is:

$$\Gamma'_{\min} = \arccos\left(\frac{{l_2}^2 + {l_3}^2 - (l_4 + l_1)^2}{2l_2 l_3}\right) \tag{7}$$

Analogous to the motion parameters of large birds in flight [9], the flapping amplitude is $\varphi = 50°$, the upper flapping limit angle is $\varphi_{max} = 45°$, and the lower flapping limit angle is $\varphi_{min} = -5°$. In order to ensure that the mechanism has better force transmission performance, the minimum transmission angle is taken as $\Gamma_{min} = 48°$, and the length of the rocker is $l_3 = 50mm$. Simultaneous formulas (2), (3), (4), (5), (6) and (7) are solved using the fsolve function in MATLAB, and the group with the most consistent data is selected. After the rounding process, the motion parameters of the flapping mechanism are obtained: the crank length is $l_1 = 21mm$, the linkage length is $l_2 = 39mm$, the rocker length is $l_3 = 50mm$, the frame length is $l_4 = 59mm$, and the frame angle is $\alpha_0 = 61°$.

3.2. Analysis of the position of the flapping mechanism

First take the inner wing mechanism as the research object for position analysis.

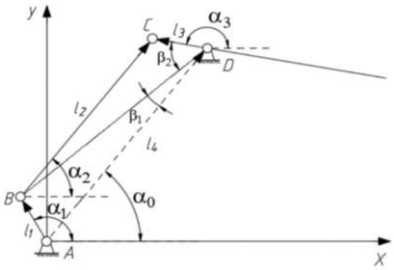

Figure 5: Diagram of inner wing mechanism

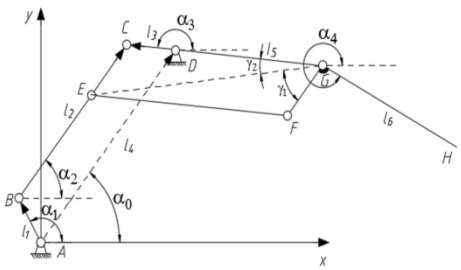

Figure 6: Diagram of outer wing mechanism

In Fig. 5, l_1 is the crank, l_2 is the linkage, l_3 is the rocker, l_4 is the frame of the crank-rocker mechanism, the angle between crank l_1 and the X axis is α_1, and the angle between linkage l_2 and the X axis is α_2. The angle between the rocker l_3 and the X axis is α_3. Rods l_1, l_2, l_3 and l_4 form a hinged four-bar mechanism. The hinged four-bar mechanism ABCD is regarded as a closed vector polygon, and $\vec{l_1}, \vec{l_2}, \vec{l_3}$ and $\vec{l_4}$ are used to represent the vector of each component, and the rotation process of the hinged four-bar mechanism at any time can be known from the principle of the mechanism. All satisfy the following closed vector equations.

$$\vec{l}_1 + \vec{l}_2 = \vec{l}_3 + \vec{l}_4 \tag{8}$$

Take their projections on the X axis and Y axis respectively to obtain the angular displacement equation in component form:

$$\begin{cases} l_1\cos\alpha_1 + l_2\cos\alpha_2 = l_3\cos\alpha_3 + l_4\cos\alpha_0 \\ l_1\sin\alpha_1 + l_2\sin\alpha_2 = l_3\sin\alpha_3 + l_4\sin\alpha_0 \end{cases} \tag{9}$$

ISSN 2616-5775 Vol. 4, Issue 6: 59-66, DOI: 10.25236/AJCIS.2021.040610

According to the geometric relations in Fig. 5 and the law of sine and cosine, it can be obtained:

$$l_{BD}{}^2 = l_1{}^2 + l_4{}^2 - 2l_1 l_4 \cos(\alpha_1 - \alpha_0) \tag{10}$$

$$\beta_1 = \arcsin\left(\frac{l_1}{l_{BD}} \sin(\alpha_1 - \alpha_0)\right) \tag{11}$$

$$\beta_2 = \arccos\left(\frac{l_{BD}{}^2 + l_3{}^2 - l_2{}^2}{2l_{BD} l_3}\right) \tag{12}$$

From formulas (10), (11) and (12), the instantaneous angular position of the rocker can be expressed as:

$$\alpha_3 = 180° + \alpha_0 - \beta_1 - \beta_2 \tag{13}$$

In order to intuitively describe the movement parameter changes of the rods, this paper uses the plot function in MATLAB to draw the movement parameter graph, and the movement relationship curve between the flutter angle position of the inner wing and the crank angle is shown in Fig. 7. It can be seen from Fig. 7 that within one rotation of the crank, the upper flapping limit angle of the inner wing mechanism is $\varphi_{max} = 45°$, and the corresponding crank angle is $268°$; the lower flapping limit angle is $\varphi_{min} = -5°$, and the corresponding crank angle is $84°$. The flapping amplitude of the inner wing mechanism is:

$$\varphi = \varphi_{\max} - \varphi_{\min} = 50° \tag{14}$$

The pole position angle is:

$$\theta = |268° - 84° - 180°| = 4° \tag{15}$$

The travel speed ratio coefficient is:

$$K = \frac{180° + \theta}{180° - \theta} = 1.05 \tag{16}$$

The minimum transmission angle is $\Gamma_{min} = 48.6°$, which meets the requirement of Γ_{min} not less than $40°$ in general mechanical transmission, indicating that the mechanism has good force transmission performance. The flapping angle and other parameters of the inner wing mechanism are basically the same as the flight motion parameters of the inner wing wings of large birds in flight.

Next, take the outer wing mechanism as the research object for position analysis. The schematic diagram of the outer wing mechanism is shown in Fig. 6. The angular position of the outer wing rod GF is:

$$\alpha_4 = \angle CGF + \angle FGH + \alpha_3 \tag{17}$$

In the formula(20), $\angle FGH$ is equal to $75°$, and connect EG to obtain:

$$\angle CGF = \gamma_1 + \gamma_2 \tag{18}$$

$$\angle BCG = \alpha_3 - \alpha_2 \tag{19}$$

$$l_{EG}{}^2 = l_{CE}{}^2 + l_{CG}{}^2 - 2l_{CE} l_{CG} \cos(\angle BCG) \tag{20}$$

$$\gamma_1 = \arccos\left(\frac{l_{EG}{}^2 + l_{FG}{}^2 - l_{EF}{}^2}{2l_{EG} l_{FG}}\right) \tag{21}$$

$$\gamma_2 = \arccos\left(\frac{l_{CG}{}^2 + l_{EG}{}^2 - l_{CE}{}^2}{2l_{CG} l_{EG}}\right) \tag{22}$$

ISSN 2616-5775 Vol. 4, Issue 6: 59-66, DOI: 10.25236/AJCIS.2021.040610

Simultaneous formulas (18), (19), (20), (21) and (22) obtain the instantaneous angular position expression of the outer wing rod GH as:

$$\alpha_4 = \gamma_1 + \gamma_2 + \alpha_3 + \angle FGH \tag{23}$$

The angular position curve diagram of the outer wing rod GH is shown in Fig. 8.

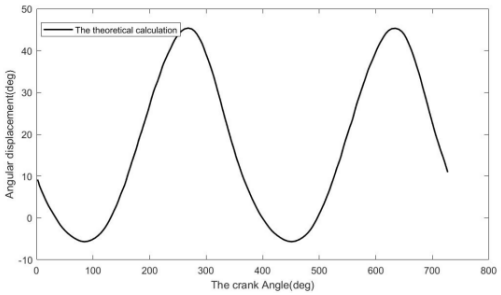

Figure 7: Curve of inner wing angle position

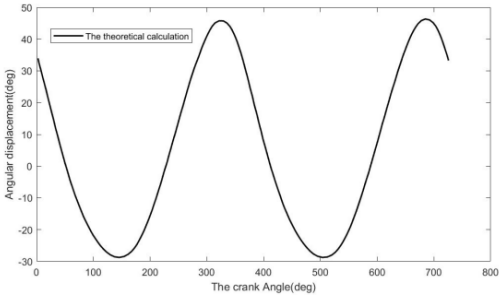

Figure 8: Curve of outer wing angle position

It can be seen from Fig. 8 that the upper flapping limit angle of the outer wing mechanism is $46°$, the lower flapping limit angle is $-28°$, and the flapping amplitude is $74°$, which is basically the same as the flapping amplitude of the outer wing wings when large birds are flying, which shows that the designed outer wing flapping mechanism has good motion characteristics.

3.3. Angular velocity analysis of flapping mechanism

In order to obtain the angular velocities of the inner wing rod CG, the angular displacement equation (12) in component form can be first obtained as a first order derivative with respect to time, and the resulting equation is expressed in matrix form as follows.

$$\begin{pmatrix} -l_2\sin\alpha_2 & l_3\sin\alpha_3 \\ -l_2\cos\alpha_2 & l_3\cos\alpha_3 \end{pmatrix} \begin{pmatrix} \omega_2 \\ \omega_3 \end{pmatrix} = \begin{pmatrix} \omega_1 l_1 \sin\alpha_1 \\ \omega_1 l_1 \cos\alpha_1 \end{pmatrix} \tag{24}$$

In formula (27), ω_1, ω_2 and ω_3 are the instantaneous angular velocities of crank l_1, linkage l_2 and rocker l_3 respectively.

Solving formula (27), the angular velocity of the rocker is:

$$\omega_3 = \frac{l_1 \sin(\alpha_1 - \alpha_2)}{l_3 \sin(\alpha_3 - \alpha_2)} \omega_1 \tag{25}$$

The graph of the angular velocity of the inner wing mechanism changing with time is shown in Figure 9. It can be seen from Fig. 9 that the maximum angular velocity of the inner wing is 10.5 *rad/s* during the up-and-down flapping. The angular velocity curve of the inner wing mechanism is relatively smooth without obvious sharp points, indicating that the inner wing mechanism is relatively stable in the flapping process.

Next, solve the instantaneous angular velocity expression of the outer wing rod GH. The first derivative of formula (23) with respect to time can be obtained:

$$\omega_4 = \dot{\gamma}_1 + \dot{\gamma}_2 + \omega_3 \tag{26}$$

The instantaneous angular velocity expression of rod CG has been obtained by formula (25).

$$\dot{\gamma}_1 = \frac{l_{CG}\cos(\alpha_3 - \alpha_2)}{l_{EG}\cos\gamma_1}(\omega_2 - \omega_3) \tag{27}$$

$$\dot{\gamma}_2 = \frac{l_{CE}\cos(\alpha_3 - \alpha_2)}{l_{EG}\cos\gamma_2}(\omega_2 - \omega_3) \tag{28}$$

Simultaneous formulas (26), (27) and (28) can obtain the angular velocity expression of the outer wing rod GH. The movement curve of the angular velocity of the outer wing rod with time is shown in

ISSN 2616-5775 Vol. 4, Issue 6: 59-66, DOI: 10.25236/AJCIS.2021.040610

Fig. 10.

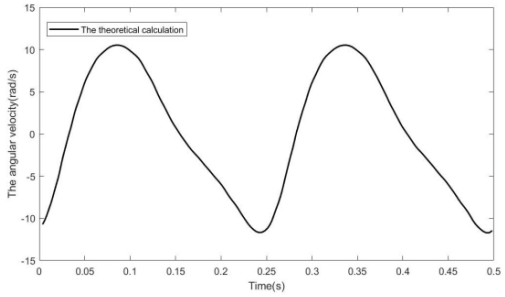

Figure 9: Angular velocity curve of inner wing

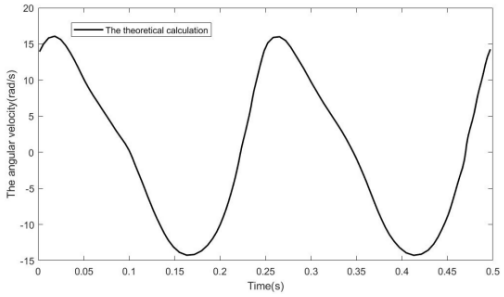

Figure 10: Angular velocity curve of outer wing

It can be seen from Fig. 10 that the maximum angular velocity of the outer wing flapping up and down is 16 *rad/s*, and there is no obvious sharp point in the angular velocity during the whole flapping period, indicating that the outer wing flapping is relatively stable.

3.4. Angular acceleration analysis of flapping mechanism

Calculating the second derivative of the angular displacement equation (9) in component form with respect to time, the following equations expressed in matrix form are obtained.

$$\begin{pmatrix} -l_2\sin\alpha_2 & l_3\sin\alpha_3 \\ -l_2\cos\alpha_2 & l_3\cos\alpha_3 \end{pmatrix}\begin{pmatrix} a_2 \\ a_3 \end{pmatrix} = \begin{pmatrix} a_1 l_1\sin\alpha_1 + {\omega_1}^2 l_1\cos\alpha_1 + {\omega_2}^2 l_2\cos\alpha_2 - {\omega_3}^2 l_3\cos\alpha_3 \\ a_1 l_1\cos\alpha_1 - {\omega_1}^2 l_1\sin\alpha_1 - {\omega_2}^2 l_2\sin\alpha_2 + {\omega_3}^2 l_3\sin\alpha_3 \end{pmatrix} \tag{29}$$

By solving the formula (29), the angular acceleration of the rocker is obtained as follows.

$$a_3 = \frac{a_1 l_1\sin(\alpha_2-\alpha_1) - {\omega_1}^2 l_1\cos(\alpha_1-\alpha_2) + {\omega_3}^2 l_3\cos(\alpha_2-\alpha_3) - {\omega_2}^2 l_2}{l_3\sin(\alpha_2-\alpha_3)} \tag{30}$$

The graph of the angular acceleration of the inner wing mechanism changing with time is shown in Figure 11. It can be seen from Fig. 11 that due to the rapid return characteristic, when the inner wing mechanism flaps upwards, the maximum angular acceleration at time $t = 0.025s$ is $440\ rad/s^2$.

Using formula (23) to calculate the second derivative with respect to time, the angular acceleration of the outer wing rod GH is obtained as:

$$a_4 = \ddot{\gamma}_1 + \ddot{\gamma}_2 + a_3 \tag{31}$$

$$\ddot{\gamma}_1 = \frac{l_{EF}\cos(\alpha_3-\alpha_2)(a_3-a_2) - l_{EF}\sin(\alpha_3-\alpha_2)(\omega_3-\omega_2)^2}{l_{EG}\cos\gamma_1} + \frac{{\dot{\gamma}_1}^2\sin\gamma_1}{\cos\gamma_1} \tag{32}$$

$$\ddot{\gamma}_2 = \frac{l_{CE}\cos(\alpha_3-\alpha_2)(a_3-a_2) - l_{CE}\sin(\alpha_3-\alpha_2)(\omega_3-\omega_2)^2}{l_{EG}\cos\gamma_2} + \frac{{\dot{\gamma}_2}^2\sin\gamma_2}{\cos\gamma_2} \tag{33}$$

Simultaneous formulas (31), (32) and (33) obtain the expression of the angular acceleration of the outer wing rod GH. The angular acceleration curve of the outer wing rod GH is shown in Figure 12.

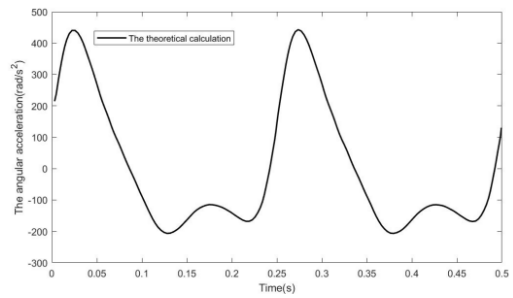

Figure 11: Angular acceleration curve of inner wing

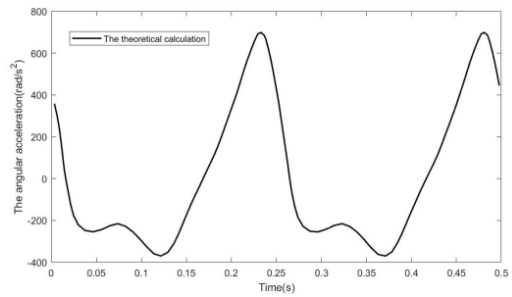

Figure 12: Angular acceleration curve of outer wing

It can be seen from Fig. 12 that due to the rapid return characteristic, when the outer wing mechanism

ISSN 2616-5775 Vol. 4, Issue 6: 59-66, DOI: 10.25236/AJCIS.2021.040610

flaps upward, the maximum angular acceleration at time t = 0.23s is $698\ rad/s^2$.

4. ADAMS Kinematics Simulation

In order to verify the correctness of the kinematic analysis of the flapping-wing mechanism, a three-dimensional model of the bionic flapping-wing mechanism can be established in SolidWorks according to the determined size parameters. At the same time, ADAMS software is used to simulate and analyze the flapping-wing mechanism. Import the 3D model into ADAMS in parasolid format, and set the material properties of each part, add motion pairs at the positions that are related to each other, and finally add driving force to the corresponding motion pairs. According to the literature [10], the flutter frequency is $f = 4Hz$, the given pinion speed is $56\pi\ rad/s$, and the angular velocity of the crank is $\omega_1 = 8\pi\ rad/s$ after the reduction gear is decelerated. The ADAMS simulation model is shown in Figure 13.

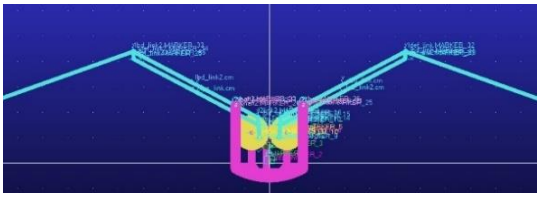

Figure 13: Adams model of flapping mechanism

After the motion simulation, by establishing reference points, check the kinematic parameter curve of the inner wing and outer wing in ADAMS/PostProcessor, and compare with the theoretical calculation values.The kinematic parameter curves in two cycles are obtained, as shown in Fig. 14.

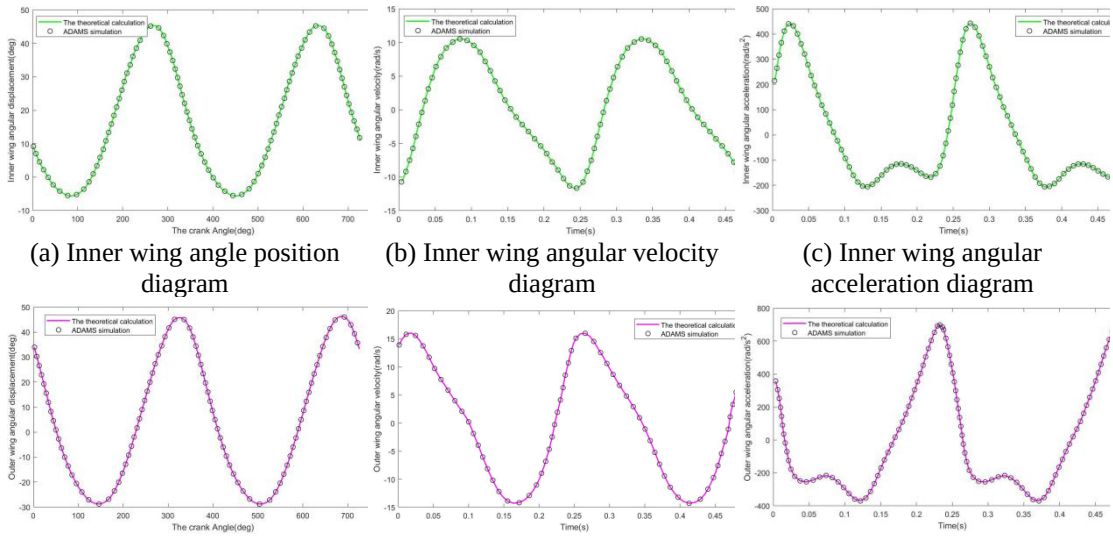

(a) Inner wing angle position diagram

(b) Inner wing angular velocity diagram

(c) Inner wing angular acceleration diagram

(d) Outer wing angle position diagram

(e) Outer wing angular velocity diagram

(f) Outer wing angular acceleration diagram

Figure 14: Comparison of theoretical calculation and ADAMS simulation output parameters

It can be seen from Fig. 14 that the motion parameter curves of the inner and outer wings obtained by ADAMS simulation are consistent with the theoretical calculation results, which proves that the two-stage flapping mechanism can well realize the expected flapping wing movement.

5. Conclusion

To better imitate the flight of large birds, this paper designs a two-stage foldable bionic flapping-wing mechanism, which achieves the completely symmetrical flapping of the left and right wings and a regular folding of the outer wing relative to the inner wing during the up and down flutter of the inner wing, thus obtaining better aerodynamic characteristics. The 3D solid modeling in SolidWorks and kinematic simulation using ADAMS led to the following conclusions:

1) During the flapping process of the flapping-wing mechanism, the upper flapping limit of the inner wing is $\varphi_{max} = 45°$ and the lower flapping limit is $\varphi_{min} = -5°$; the upper flapping limit of the outer

ISSN 2616-5775 Vol. 4, Issue 6: 59-66, DOI: 10.25236/AJCIS.2021.040610

wing mechanism is $\varphi_{max} = 46°$, and the lower flapping limit is $\varphi_{min} = -28°$, which are consistent with the flight motion parameters of large birds.

2) The minimum transmission angle of the flapping wing mechanism is $\Gamma_{min} = 48.6°$, which has good power transmission performance.

3) Using ADAMS software to simulate and analyze the flapping-wing mechanism, the kinematic parameter curves of the inner and outer wings are consistent with the theoretical calculation results, which verifies the correctness of the theoretical analysis.

References

[1] DICKINSON M H, LEHMANN F O, SANE S P. Wing rotation and the aerodynamic basis of insect flight [J]. Science, 1999, 284(5422): 1954-1960.
[2] LIU H. An introduction to flapping wing aerodynaimcs [M]. New York: Cambridge University Press, 2013.
[3] LIU H, RAVI S, KOLOMENSKIY D, et al. Biomechanics and biomimetics in insectinspired flight systems [J]. Philosophical Transactions of the Royal Society B Biological Sciences, 2016, 371(1704): 20150390.120150390.11.
[4] Liu Lan, Fang Zongde. Bionic design and technology research of flapping-wing miniature aircraft [D]. Xi'an: Northwestern Polytechnical University, 1999: 21-24.
[5] PORNSIN-SIRIRAK TN, TAI Y C, HO C M, et al. Microbat: apalm-sized electrically powered ornithopter [C]// Proceedings of the NASA/JPL Workshop on Biomorphic Robotics. Pasadena, US: NASA, 2001: 14-17.
[6] Tobalske B, Dial K. Flight Kinematics of Black-Billed Magpies and Pigeons over a Wide Range of Speeds [J]. Journal of Experimental Biology, 1996, 199(2): 263-280.
[7] Shyy W, Berg M, Ljungqvist D. Flapping and flexible wings for biological and micro air vehicles [J]. Progress in Aerospace Sciences, 1999.
[8] XU Yicun, ZONG Guanghua, BI Shusheng, YU Jingjun. Design analysis of space crank rocker flutter wing configuration [J]. Journal of Aerodynamics, 2009, 24(01), pp. 204-208.
[9] Wu Rui. Design and experimental research of two-stage flexible bird flapping-wing aircraft prototype [D]. Harbin Institute of Technology, 2019.
[10] Liu Cong. Research on the structure design and dynamics simulation of the bionic flapping-wing aircraft [D]. Harbin Institute of Technology, 2010.